X-ray Ejecta, White Light CMEs and a Coronal Shock Wave

N. Gopalswamy[1], O. C. St. Cyr[1,2], M. L. Kaiser[3], and S. Yashiro[1]

[1]Center for Solar Physics and Space Weather, The Catholic University of America, Washington DC 20064
[2]Also at Computational Physics Inc., Virginia
[3]Code 695.0 NASA Goddard Space Flight Center, Greenbelt, MD 20771, USA

Abstract

We report on a coronal shock wave inferred from the metric type II burst of 1996 January 13. To identify the shock driver, we examined mass motions in the form of X-ray ejecta and white light coronal mass ejections (CMEs). None of the ejections could be considered fast (> 400 km s^{-1}) events. In white light, two CMEs occurred in quick succession, with the first one associated with an X-ray ejecta near the solar surface. The second CME started at an unusually large height in the corona and carried a dark void in it. The first CME decelerated and stalled while the second one accelerated, both in the coronagraph field of view. We identify the X-ray ejecta to be the driver of the coronal shock inferred from metric type II burst. The shock speed reported in the Solar Geophysical Data (1000-2000 km s^{-1}) seems to be extremely large compared to the speeds inferred from X-ray and white light observations. We suggest that the MHD fast-mode speed in the inner corona is low enough that the X-ray ejecta is supermagnetosonic and hence can drive a shock to produce the type II burst.

1 Introduction

After the advent of the Solar and Heliospheric Observatory (SOHO) mission, coronal mass ejections (CMEs) have been studied quite extensively over a significant volume of the Sun-Earth connected space. These studies have greatly benefited from X-ray, EUV and microwave observations which provide information on the initiation of CMEs near the solar surface. Heating and expansion of filaments, coronal arcade formation and coronal dimming are some of the features seen at these wavelengths which tell us about the CME onset phase (see e.g., Hudson, 1999; Gopalswamy, 1999; Hanaoka and Shinkawa, 1999; Hudson and Webb, 1997; Gopalswamy and Hanaoka, 1998; Thompson et al, 1998). Metric radio bursts are signatures of nonthermal particle production during the eruptive events. Type II radio bursts in the metric to kilometric wavelength regimes are indicative of large-scale coronal and interplanetary shocks whose exact relationship to the eruptive events is not fully understood (see e.g., Cane, 1984; Kahler et al, 1984; Bougeret, 1985; Gopalswamy et al, 1998; Kaiser et al., 1998; Cliver, 1999). One of the possible shock-drivers recently proposed by Gopalswamy et al. (1997) is the X-ray ejecta during solar eruptions. This suggestion is supported by recent studies (Klein et al., 1999; Klassen et al, 1999; Gopalswamy et al., 1999a) which combine radio and X-ray observations. How the X-ray ejecta is related to the white light CME is poorly understood (Nitta and Akiyama, 1999). We had an opportunity to address this issue in connection with the January 13, 1996 CME, one of the earliest events observed by the SOHO mission. This event occurred on a quiet day with no active center on the disk. This enabled us to study the event without any confusion from other activities. The event consisted of coronal dimming, X-ray ejecta, a set of white light CMEs and metric radio bursts. Another motivation for studying this event is the occurrence of a metric type II radio burst implying a fast mode shock despite the low speed ($\sim$ 200 km s^{-1}) of all observed mass motions. We also discuss the possibility of CME initiation/acceleration from the outer corona.

2 Observations and Analysis

The 1996 January 13 eruption occurred from behind the west limb. An active region (AR) complex consisting of NOAA ARs 7939 (N10 W90) and 7937 (S03 W90) were present close to the west limb at the beginning of January 12. The two regions were located on either side of the equator, separated by $\sim 13^\circ$ in latitude. We expect the AR complex to be $\sim 25^\circ$ behind the limb at the time of the eruption in question. Both regions produced surges frequently (Solar Geophysical Data, January 1996). Table 1 provides a brief summary of various activities associated with the event: Soft X-ray dimming, white light CME and metric radio emission. In the metric domain, type III bursts were followed by a type II burst.

2.1 X-ray Observations

The Soft X-ray Telescope (SXT, Tsuneta et al, 1991) on board *Yohkoh* spacecraft observed the eruptive event in full frame images. The best coverage of the event was obtained with the sandwich filter. The quarter-resolution SXT images obtained during the eruption have a pixel size of $\sim$ 9.84 arcsec. The image cadence was not very good, but was sufficient to track the slow eruption and to determine the morphological properties. The X-ray event consisted of a

prolonged dimming of the X-ray structures and a large-scale ejection from the equatorial region above the west limb.

A series of X-ray images, actual and differenced, are shown in Fig. 1. The dimming started as early as 17:26 UT on January 13, 1996 and increased with time. The dimming reached its maximum level at about 19:25 UT and remained at the same level when the satellite emerged from its night around 20:08 UT. The dimming region covered a position angle extent of 23°, starting from N08 to S15 at 20:15 UT, and extended up to a height of 0.12 $R_\odot$ above the limb for a period of about 3 hours. Since there was no other active region on the disk, the observed X-ray flux is mostly from the west limb. The dimming could have been caused by the eruptive structures as well as by rotation of the west limb structures. In order to see this, we have plotted the X-ray light curves in four locations above the west limb for the period January 11-14, 1997 (see Fig. 2a). The locations are marked by the boxes in Fig. 2b. The structure within box D was quiet and was the first to rotate behind the limb, as seen from the monotonic decrease in X-ray intensity. The boxes A-C correspond to the region of eruption. The X-ray intensity in A-C start declining as the regions start rotating behind the limb from the beginning of January 12. However, the light curves are heavily modulated by activity and hence do not show a monotonic decrease in intensity, making it difficult to separate the dimmings due to eruption and rotation.

2.1.1 Large-scale X-ray Ejecta

A sudden ejection was observed by SXT starting after 20:15 UT on January 13 (see Fig. 2a, light curve A). The difference images at 20:15 and 20:24 UT in Fig. 3 show the onset of the X-ray ejection. The ejection began within the dimming region, covering a position angle range of $\sim 15°$ bracketed by the equator to the north and S15. After this time, the ejection expanded to a larger volume, as can be seen in the 20:28 UT image in Fig. 1. The ejection consisted of a large scale loop-like structure, covering about 30° in position angle and a smaller cusp-shaped structure at the southern end of the large-scale structure. The loop structure moved out of the field of view by 20:49 UT. We determined the speed of the ejecta based on the two frames (20:15 UT and 20:24 UT) in which the motion of the ejecta was discernible. At 20:24 UT, the ejection was at a height of 0.16 $R_\odot$. Unfortunately, we do not have images between 20:15 and 20:24 UT. Assuming that the ejection was close to the solar surface at 20:15 UT, we can get a lower limit to the speed as ~ 206 km s^{-1} in the plane of the sky.

2.2 White Light Observations

White light observations were obtained by the SOHO mission's Large Angle and Spectrometric Coronagraph (LASCO, Brueckner et al., 1995) with a high image cadence (once every 3 minutes). The outermost coronagraph (C3) of LASCO covers a heliocentric distance range of ~ 3.6 to 30 $R_\odot$. No significant changes were detected above the west limb from the beginning of January 11 until about 21:47 UT on January 13. Fig. 4 shows a series of images from 21:47 UT (January 13) to 09:20 UT (January 14) describing the evolution of the corona above the west limb. A narrow brightening appeared above the occulting disk of the C3 coronagraph in the 21:52 UT image (marked 2 in the 23:20 UT image), preceded by a faint void (marked 1). The brightening slowly extended to larger heights without significant expansion in the lateral direction. Features 1 and 2 seem to be the substructures of a CME with no obvious frontal structure. We refer to this CME as the first CME (CME1). By 23:41 UT, the brightening of CME1 had extended to

a height of about 5.5 $R_\odot$ with no further increase in height. Around this time, a new feature appeared from below the the bright feature of CME1. This new feature (marked 3 in the 05:38 UT image) was followed by a circular dark void (marked 5). We refer to the new feature along with the void as the second CME (CME2). CME2 is a narrow, cone-shaped ejection with a slow expansion. By $\sim$ 04:01 UT on January 14, CME2 acquired an unusual shape (like a candle flame) with its base at the occulting disk narrower than the middle section where the void was located. The void expanded steadily, maintaining the circular shape (the outer and inner edges of the void are marked as 4 and 6 in the 05:38 UT image). Thus, two CMEs were observed in quick succession.

The height-time history in Fig. 5 shows that the trajectories of CME1 and CME2 were distinct: Both substructures of CME1 decelerated while the leading edge of CME2 accelerated. The void of CME2 moved with constant speed. We compare the height-time histories of the bright feature of CME1 (trajectory 2 in Fig. 4) with the leading edge of CME2 (trajectory 3 in Fig. 4) by fitting second degree polynomials (constant acceleration):

$$h_2 = 9.68 \times 10^{-2} + 6.19 \times 10^{-4} t - 1.16 \times 10^{-8} t^2 \quad (1)$$

for substructure 2 of CME1 and,

$$h_3 = 3.73 - 2.82 \times 10^{-5} t + 6.62 \times 10^{-9} t^2 \quad (2)$$

for substructure 3 of CME2. In equations (1) and (2), h_2 and h_3 are heliocentric distances in $R_\odot$ and t is time in seconds from 20:00 UT on January 13, 1996. The substructure 2 had a deceleration of 16.1 m s^{-2}, while 3 showed an acceleration of 9.2 m s^{-2}. The average speed of CME1 was $\sim$ 258 km s^{-1} (based on feature 2). CME2 accelerated to $\sim$ 280 km s^{-1} by the time it reached a height of $\sim$ 9 $R_\odot$ while it was very slow ($\sim$ 100 km s^{-1}) when CME1 started stalling. There is no real solution of equation (2) for $h_3 = 1$ because the starting height of the trajectory is $\sim$ 3.7 $R_\odot$ (obtained by setting the speed to zero (dh_3/dt = 0 in equation (2)).

The void of CME2 had a constant speed of $\sim$ 254 km s^{-1}. The void had an initial diameter of $\sim$ 1.5 $R_\odot$ at 04:30 UT (January 14) and expanded to $\sim$ 2.25 $R_\odot$ at 09:00 UT. The expansion rate (23 km s^{-1}) is much smaller than the radial speed, and is of the same order of magnitude as the typical expansion rate ($\sim$ 51 km s^{-1}) of flux ropes (Chen, 1997). The void could be interpreted as a flux-rope structure slowly expanding as it propagated away from the Sun. Since the eruption is from the transequatorial region, it is difficult to imagine a pre-formed flux rope as in the case of streamer disruption events (Low and Hundhausen, 1995). However, there is an alternative model (Gosling, 1990), according to which the flux rope is formed out of the frontal arcade due to reconnection.

Following these events, a faster and wider ($\sim$ 56°) CME occurred on January 15, 1996 at 07:01 UT (see Howard et al., 1997). There was no other CME from the west limb for the next two weeks. The January 15 CME was complex, with substructures moving at various speeds from 228 to 573 km s^{-1}, and also had a void similar to CME2. There was a progressive increase in the width of the successive CMEs suggesting that magnetic fields from a larger volume of the corona became open after successive CMEs.

The clear deceleration of CME1 is a rare case because most CMEs show either positive or no acceleration in the inner corona (Howard et al, 1997; St. Cyr et al., 2000)). Sheeley et al.

(1999) made a detailed study of CME speeds comparing broadside and head-on observations. They found that typically slow CMEs which were accelerating, and fast CMEs that had constant speed within the coronagraph field of view. While CME2 is an accelerating slow event, CME1 is clearly an exception. It is not clear if this peculiar combination of decelerating and accelerating CMEs in quick succession is due to the interaction between the two CMEs, recently identified in the LASCO field of view (Gopalswamy et al. 2001). Sheeley et al. (1999) suggested that shock waves ahead of fast CMEs sweep up material from the corona causing the CMEs to slow down. In the present case, we do have a shock associated with CME1, but there is no evidence for swept up material because CME1 does not show a frontal structure. Moreover, the region of deceleration inferred by Sheeley et al. is far beyond the coronal region in which CME1 decelerates.

2.3 Nonthermal Phenomena: Radio Bursts

A metric type II burst was reported by several radio observatories. The burst started at 20:29 UT at 42 MHz and ended at 20:32 UT at 28 MHz. Since the ending frequency is close to the lowest frequency observable from most ground-based radio telescopes, we examined the dynamic spectrum in the frequency range 1-14 MHz, obtained by the Radio and Plasma Wave Experiment (WAVES) on board the Wind mission. No type II burst was found in the WAVES spectral domain, suggesting that the type II burst ended somewhere between 28 and 14 MHz. Fast-mode MHD shocks propagating through the corona and interplanetary medium are thought to produce radio emission at the local plasma frequency and its harmonic. For events occuring on the solar disk, metric type II bursts exhibit both fundamental (at the local plasma frequency) and harmonic (at twice the local plasma frequency) components. For limb events, mostly the harmonic component is observed because the fundamental is occulted by the overlying corona. If we assume harmonic emission for the observed type II radio burst, the starting frequency of 42 MHz corresponds to a local plasma frequency of 21 MHz.

The metric type II burst was preceded by metric type III bursts from 20:14 to 20:21 UT in the frequency range 45 - 25 MHz. The type III bursts signal the onset of flares and the availability of open magnetic field lines along which energetic electrons propagate. The onset of metric type III onset coincides with the rapid increase in GOES X-ray flux as well as in the X-ray flux measured from the region of interest in the SXT images. The type III bursts also started roughly at the same frequency as the type II burst (42 MHz) which is an indication that the plasma levels at frequencies higher than 42 MHz were occulted by the limb. Since the activity center was less than 25° behind the limb, we think that the 21 MHz plasma level, where the type II burst seem to have started, is relatively low-lying.

3 Relation between X-ray and White Light Ejections

The two well-defined phases (dimming and ejecta) in X-rays are temporally and spatially close to CME1 in white light. Setting $h_2 = 1$ in equation (1) gives an onset time of 20:25 UT for CME1, roughly corresponding to the time of the X-ray ejecta (see Fig. 1). The single height measurement for the X-ray ejecta is shown in Fig. 5, which lines up well with the substructures of CME1. Note that this onset time has to be an upper limit because the structure has to accelerate initially (We ignore the small projection effect). Thus, the bright substructure of

CME1 is likely to be the white-light counterpart of the X-ray ejecta. Gopalswamy et al. (1997) found a very similar case in which a fast X-ray ejecta closely followed a white light CME.

The void of CME1 was of poor contrast, so we could not measure its height during the early phase. We associate the X-ray dimming (around 19:15 UT) with the onset of CME1. The earlier prolonged dimming may be partly due to solar rotation and partly due to the pre-eruption depletion as in the 1997 April 27 event reported by Gopalswamy et al. (1999b). The remarkably similar transequatorial dimming during the 1998 April 27 disk event was observed in X-rays and EUV and was not due to solar rotation. In the present event, ARs 7939 and 7937 also had transequatorial structure but behind the west limb. This makes it very difficult to separate dimming due to rotation from the true evacuation of the corona.

4 Flare, CME, and Coronal Shock

Figure 6 compares soft X-ray light curves from SXT and GOES for a period including the eruption. We chose a rectangular box covering the dimming region and computed the average X-ray flux per pixel within this box. The flux is normalized to the initial value at 16:54 UT and we have plotted the deviation from this initial value in Fig. 6. The flux drops by $\sim 32\%$ at the deepest levels (19:15 UT). In spite of the poor cadence, the SXT curve shows changes corresponding to the three spurts of activity seen in GOES. The correspondence is rather good for the main event starting at $\sim$ 20:15 UT. Since there is no other activity on the disk, we can safely identify the GOES enhancement at this time with the X-ray ejection observed by the SXT. The good agreement between the GOES and SXT light curves suggests a flare close to the limb starting at $\sim$ 20:14 UT, consistent with the metric type III activity. Since the type III electrons get to the outer corona in a few seconds, it is safe to assume that the flare onset is at 20:14 UT. The X-ray ejecta was first seen above the limb at 20:24 UT. In section 2.1.1 we estimated a lower limit to the X-ray ejecta speed as 206 km s^{-1}. Since the event was from behind the limb, a slightly earlier onset cannot be ruled out.

The metric type II burst started at 20:29 UT with a starting frequency of 42 MHz. Assuming harmonic emission, we expect the projected height of the 21 MHz plasma level to be close to the limb, since frequencies higher than 42 MHz were probably occulted. If the X-ray ejecta were the driver of the shock, it is expected to be in the vicinity of the 21 MHz plasma level around 20:29 UT. The X-ray ejecta was close to the limb around the time of the type II burst, so it is a likely candidate provided it was fast enough to drive a shock. The speed of the X-ray ejecta was $\sim$ 206 km s^{-1}, close to the average speed (258 km s^{-1}) of CME1 (bright feature). Only mass motions with speeds $>$ 400 km s^{-1}, are thought to be associated with type II bursts (Gosling et al., 1976). The speed of the X-ray ejecta in the event in question seems very low to drive a shock. However, Gopalswamy et al. (2001) showed that the magnetosonic speed outside of active regions could be as low as 200 km s^{-1}, so that weak fast-mode shocks with speeds slightly more than 200 km s^{-1} can propagate in the low corona. The fast-mode speed, however, increases with height and peaks in the 2-3 $R_\odot$ range which might destroy most of the low Mach number shocks (see also Mann et al. 1999).

The shock speed in the present event reported in the Solar Geophysical Data (SGD) ranged from 1000 km s^{-1} (Sagamore Hill) to 2000 km s^{-1} (Palehua). None of the motions observed in X-rays or white light had speeds anywhere near the 1000 to 2000 km s^{-1} reported in SGD. Speeds such as these derived from the radio spectra, depend on the coronal density model assumed and

the proper identification of the emission harmonic. The model also needs to be normalized to the coronal base density. Moreover, radial propagation of the shock is usually assumed, which may not be true (see, e.g., Gopalswamy et al., 2000). Thus, the reported in SGD may be off by a large factor. In the present case, the reported speeds seem to be 5-10 times larger than what X-ray and white-light mass motions imply. An alternative interpretation of the type II burst is to invoke the blast wave scenario. While we cannot rule out the possibility of a fast blast wave, there is no independent way of confirming it. This difficulty led Gopalswamy et al. (1998) to suggest a short-lived driver as the source of coronal shock (meaning it is capable of driving a shock only over a short period). We identified the X-ray ejecta with CME1 which decelerated and stalled at a height of about 6 $R_\odot$. The short lifetime of the metric type II burst is also consistent with the deceleration of CME1. It must, however, be pointed out that there is disagreement regarding the association of type II shocks with decelerating mass motions (Cliver, 1999; Gopalswamy et al, 1999c; Garczynska, 1991).

5 Summary and Conclusions

We have reported on the 1996 January 13 metric type II burst associated with a set of white-light CMEs and an X-ray ejecta on 1996 January 13. The decelerating and stalling first CME was associated with the X-ray ejecta, while there was no obvious near-surface signatures of the accelerating, second CME. This event was observed with very high time cadence by the LASCO/C3 coronagraph, so we were able to study the detailed evolution of the CMEs. The specific conclusions of this study are:

(i) The X-ray ejecta is the most probable driver of the coronal shock wave. The second of the two white light CMEs accelerated and attained a speed of only ~ 280 km s^{-1} several hours after the type II burst. No frontal structure was observed for the first CME. Even though all the substructures of the first CME were decelerating, the mass motions in the inner corona were fast enough to drive a fast-mode shock; this is primarily because the magnetosonic speed at the periphery of active regions in the inner corona could be sufficiently low.

(ii) None of the mass motions observed in X-rays and white light were fast (> 400 km s^{-1}), contrary to the high speeds (1000 to 2000 km s^{-1}) reported in the Solar Geophysical data. This is a very good example of a slow CME associated with metric type II burst. The radial profile of the fast-mode speed seems to be playing a decisive role in the occurrence of the coronal shock.

(iii) The white-light observations suggest the possibility of a partial eruption followed by a full eruption: the first CME stopped at a height of ~ 6.0 $R_\odot$ while the second one accelerated from a height of about 4 $R_\odot$. There was no near-surface counterpart of the second CME and hence might have started from an unusually large height; otherwise the second CME is similar to most of the accelerating CMEs. However, there was no white-light observations at heights below the occulting disk of the C3 coronagraph, so we cannot confirm this.

(iv) There was a series of CMEs from the same position angle and the successive CMEs had an increasing width. All these CMEs originated from the same transequatorial region, and contained conspicuous voids which could be interpreted as flux rope structures.

Acknowledgements

This work was supported in part by grants from NASA (NAG5-6139, NCC5-8998 and the ISTP/SOLARMAX program), NSF (Space Weather Program ATM9819924) and the Air Force Office of Scientific Research (F49620-00-1-0012). We thank J. B. Gurman for SDAC data and

T. Moran for comments on the manuscript. The Soft X-ray Telescope (SXT) on Yohkoh was built by the Lockheed Solar and Astrophysics Laboratory in collaboration with the National Astronomical Observatory of Japan, and the University of Tokyo, with the support of NASA and ISAS. SOHO is a mission of international cooperation between ESA and NASA. We acknowledge the comments of the anonymous referee which helped improve the presentation of the paper.

References

Bougeret, J.-L.. 1985: in B. T. Tsurutani and R. G. Stone (eds.), *Collisionless Shocks from the Heliosphere: Reviews of Current Research*, American Geophysical Union, Washington DC, p. 13.

Brueckner, G. E., et al.: 1995, Solar Phys., **162**, 357.

Cane, H. V.: 1984, Astron. Astrophys., **140**, 205.

Chen, J.: 1997, in N. Crooker, J. A. Joselyn and J. Feynman (eds.), *Coronal Mass Ejections*, Geophysical Monograph 99, American Geophysical Union, Washington DC, p. 65.

Cliver, E. W.: 1999, J. Geophys. Res., **107**, 4748.

Garczynska, I. N.: 1991, Solar Phys., **131**, 129.

Gopalswamy, N. 1999: in T. Bastian, N. Gopalswamy, and K. Shibasaki (eds.), *Solar Physics from Radio Observations*, NRO Report 479, Nobeyama Radio Observatory, Nobeyama, Japan, p. 141.

Gopalswamy, N. and Hanaoka, Y.: 1998, Astrophys. J., **498**, L179. Gopalswamy, Gopalswamy, N., et al.: 1998, J. Geophys. Res., **103**, 307.

Gopalswamy, N., Kundu, M. R., Manoharan, P. K., Raoult, A., Nitta, N. and Zarka, P. : 1997, Astrophys. J., **486**, 1086.

Gopalswamy, N., Nitta, N., Manoharan, P. K. Raoult, A. and Pick, M.: 1999a, Astron. Astrophys., **347**, 684.

Gopalswamy, N., Kaiser, M. L., MacDowall, R. J., Reiner, M. J., Thompson, B. J., and St. Cyr, O. C.: 1999b, in S. R. Habbal, R. Esser, J. V. Hollweg, and P. A. Isenberg (eds.), *Solar Wind Nine*, AIP conference Proceedings 471, p. 641.

Gopalswamy, N., et al.: 1999c, J. Geophys. Res., **104**, 4749.

Gopalswamy, N., Yashiro, S., Kaiser, M. L., Howard, R. A. and Bougeret, J.-L.: 2001, Astrophys. J., **548**, L91.

Gopalswamy, N., Lara, A., Kaiser, M. L., and Bougeret, J.-L.: 2001, J. Geophys. Res., in press, 2001.

Gosling, J. T.: 1990, in C. T. Russell, E. R. Priest, and L. C. Lee (eds.), *Physics of Magnetic Flux Ropes*, Geophys. Monogr. Ser., Vol. 58, American Geophysical Union, Washington, D. C., p. 343.

Gosling, J. T., Hildner, E., MacQueen, R. M., Munro, R. H., Poland, A. I., and Ross, C.: 1976, Solar Phys., **48**, 389.

Hanaoka, Y. and Shinkawa, T.: 1999, Astrophys. J., **510**, 466.

Howard, R. A. et al.: 1997, in N. Crooker, J. A. Joselyn, and J. Feynman (eds.), *Coronal Mass Ejections*, AGU Monograph 99, American Geophysical Union, Washington D. C., p. 17.

Hudson, H. S.: 1999, in T. Bastian, N. Gopalswamy, and K. Shibasaki (eds.), *Solar Physics from Radio Observations*, NRO Report 479, Nobeyama Radio Observatory, Nobeyama, Japan, p. 159.

Hudson, H. S. and Webb, D. F.: 1997, in N. Crooker, J. A. Joselyn and J. Feynman (eds.), Coronal Mass Ejections, Geophysical Monograph 99, American Geophysical Union, Washington DC, p. 27.

Kahler, S. W., Sheeley, N. R., Howard, R. H., Michels, D. J., and Koomen, M. J.: 1984, Solar Phys., **93**, 133.

Kaiser, M. L. et al.: 1998, Geophys. Res. Lett., **25**, 2501.

Klassen, A., Aurass, H., Klein, K.-L., Hofmann, A. and Mann, G.: 1999, Astron. Astrophys., **343**, 287.
Klein, K.-L., Khan, J. I., Vilmer, N., DeLouis, J.-M., and Aurass, H.: 1999, Astron. Astrophys., **346**, L53.
Low, B. C. and Hundhausen, A. J.: 1995, Astrophys. J., **443**, 818.
Mann, G., Aurass, H., Klassen, A., Estel, C., and Thompson, B. J.: 1999, in J.-C. Vial and B. Kaldeich-Schurmann (eds.), *Plasma Dynamics and Diagnostics in the Solar Transition Region and Corona*, ESA SP-446, p. 477.
Nitta, N. and Akiyama, S.: 1999, Astrophys. J., **525**, L57.
Sheeley Jr., N. R. Walters, J. H., Wang, Y.-M., and Howard, R. A.: 1999, J. Geophys. Res., **104**, 24739.
St. Cyr, O. C. et al.: 2000, J. Geophys. Res., **105**, 18169.
Sterling, A., Hudson, H. S. and Watanabe, T.: 1997, ApJ, **479**, L149.
Thompson, B. J., Plunkett, S. P., Gurman, J. B., Newmark, J. S., St. Cyr, O. C., Michels, D. J.: 1998, Geophys. Res. Lett., **25**, 2465.
Tsuneta, S. et al.: 1991, Solar Phys. **136**, 37.

Table 1: Timeline of the January 13, 1996 Eruptive Event

UT	Activity
17:00	Onset of X-ray Dimming
20:08	Maximum Dimming
20:14 - 20:21	Metric Type III bursts (45 - 25 MHz
20:15 - 20:24	Onset of X-ray ejecta
20:29 -20:32	Metric Type II burst (42 - 25 MHz)
21:57	Onset of First CME in C3 FOV at 3 $R_{\odot}$
23:51	Onset of second CME at 3.7 $R_{\odot}$

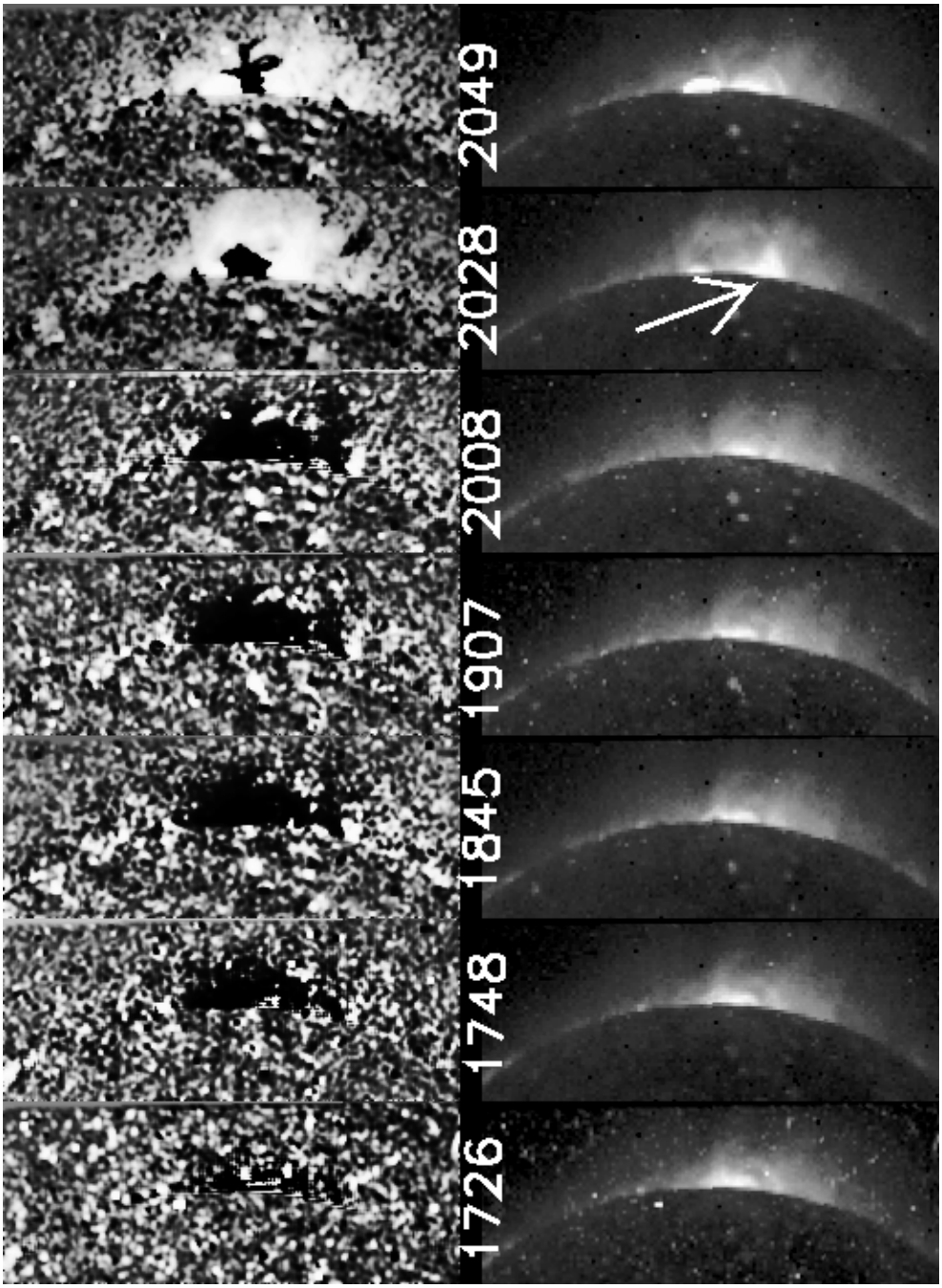

Figure 1: A series of X-ray images from *Yohkoh's* Soft X-ray Telescope (SXT) showing the ejecta from above the west limb between 17:26 and 20:49 UT on January 13, 1996. In the top panel, we have shown difference images with a suitable base image in the pre-event stage subtracted. In the bottom panel we have shown the actual images. The arrow points to a cusp-shaped region that appeared along with the X-ray ejecta. The marked times are common for both top and bottom panels. North is to the top and east is to the left here and in all the images shown in this paper.

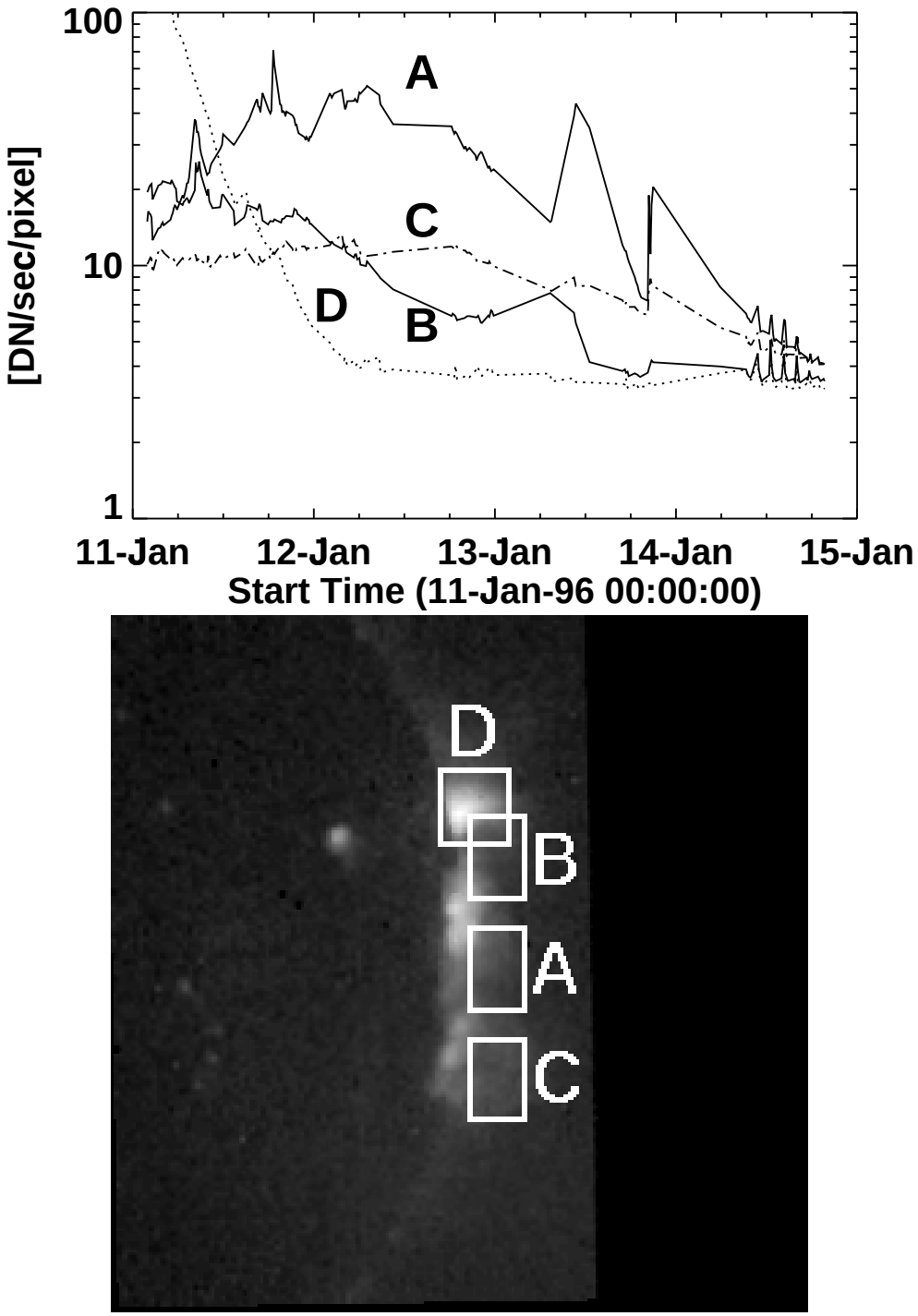

Figure 2: (a) Average X-ray intensities (in units of data number (DN) per second per pixel) in four subregions at the west limb, marked A, B, C, and D in (b). A and B are within the main dimming region. D is an isolated structure to the north of the region of eruption. C is just to the south of the eruption.

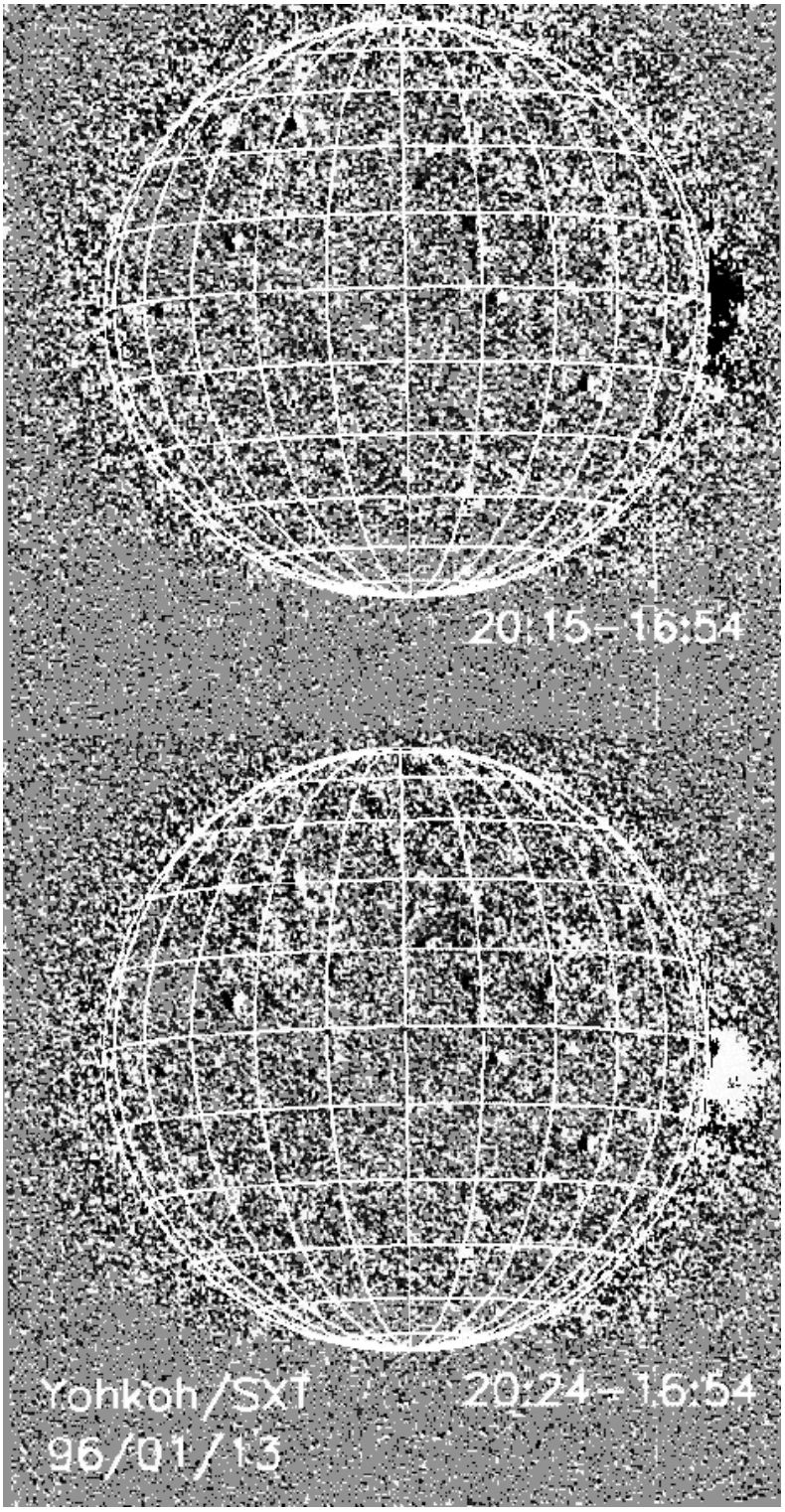

Figure 3: Full disk difference images from *Yohkoh*/SXT at 20:15 (top) and 20:24 UT (bottom) showing the onset of the bright X-ray ejecta nearly covering the dimming (dark) region.

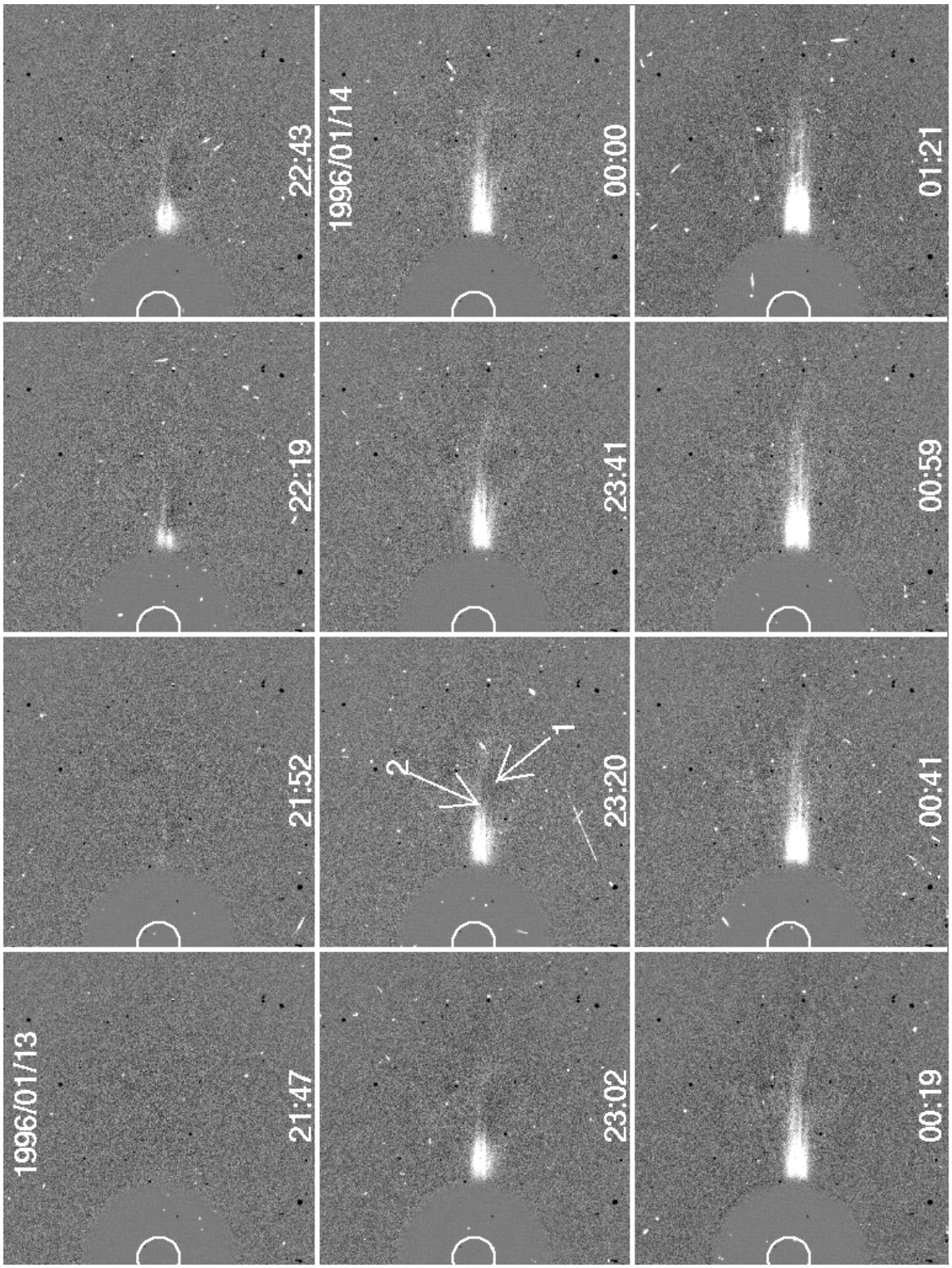

Figure 4: A series of white light (SOHO/LASCO) images showing all the changes above the west limb for January 13-14, 1997. The substructures 1 and 2 of CME1 (January 13 23:20 UT) and 3-6 of CME2 (January 14 05:38 UT image) are marked by arrows.

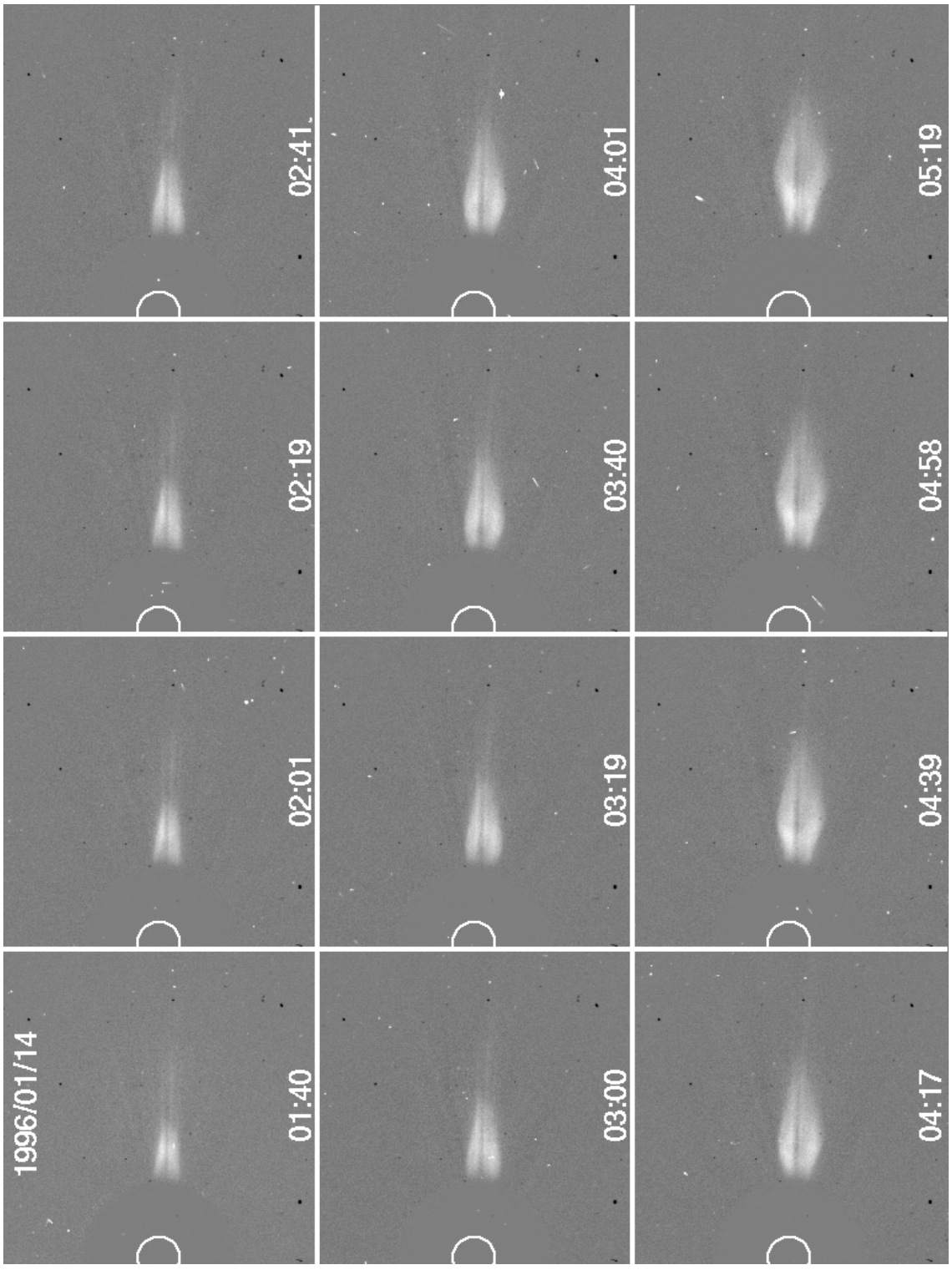

Figure 4 (Cont.)

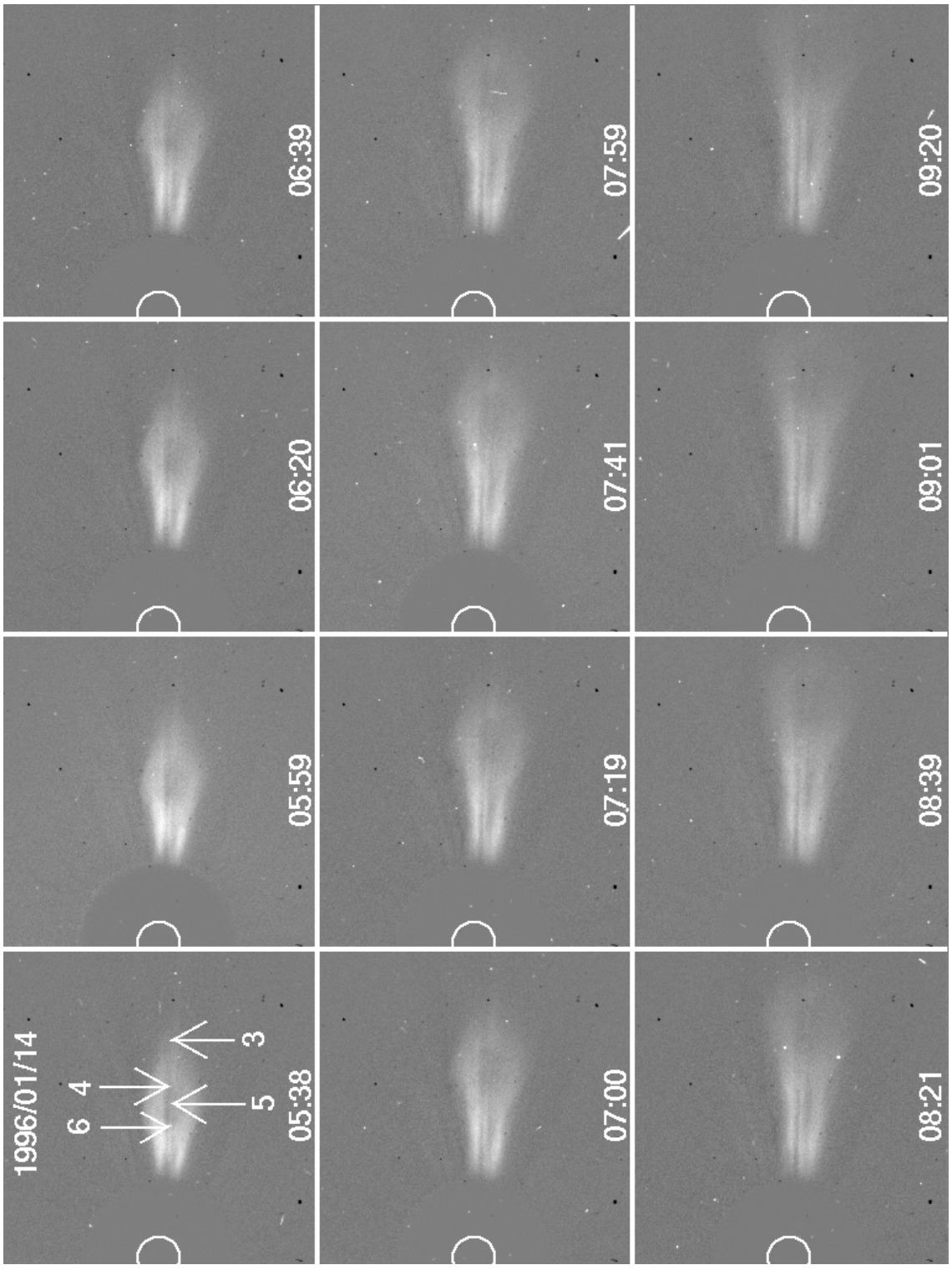

Figure 4 (Cont.)

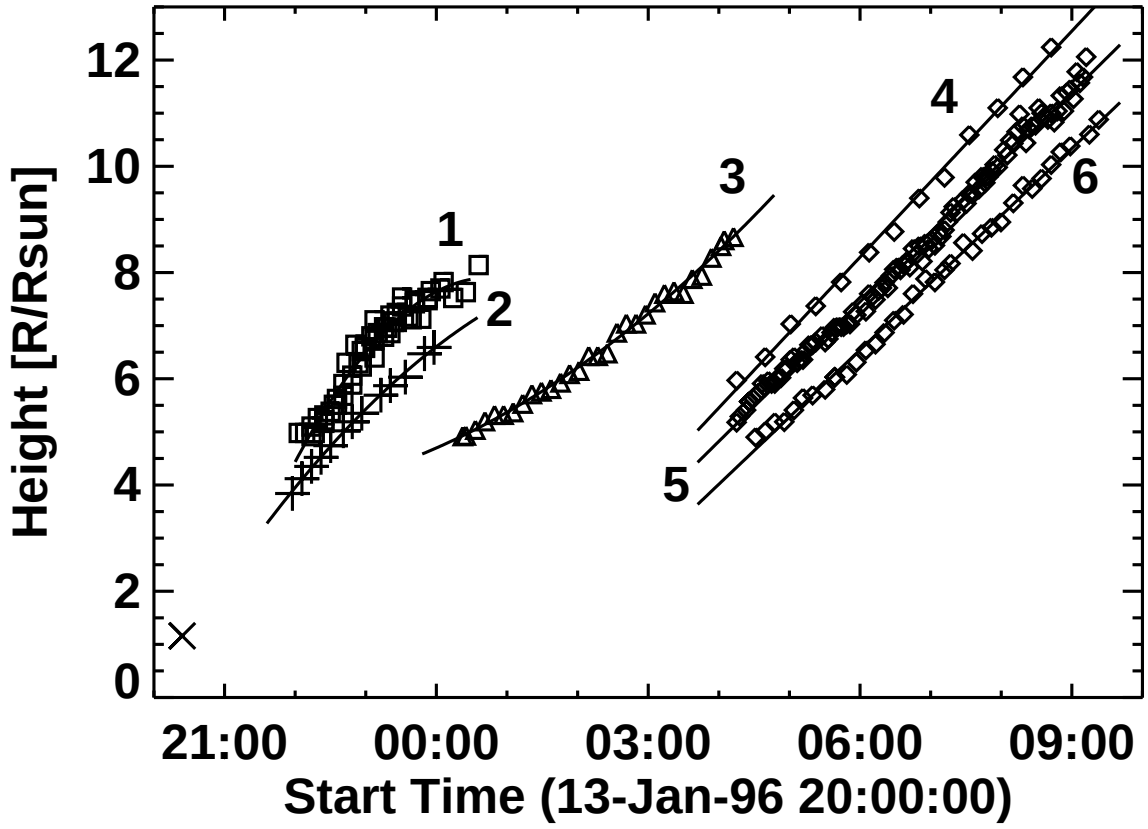

Figure 5: Height-time plot of the two CMEs as measured from LASCO/C3 images. The numbers 1-6 correspond to various substructures marked in Fig. 4. The solid lines through the data points are the constant-acceleration (features 1-2) and constant speed (features 4-6) fits.

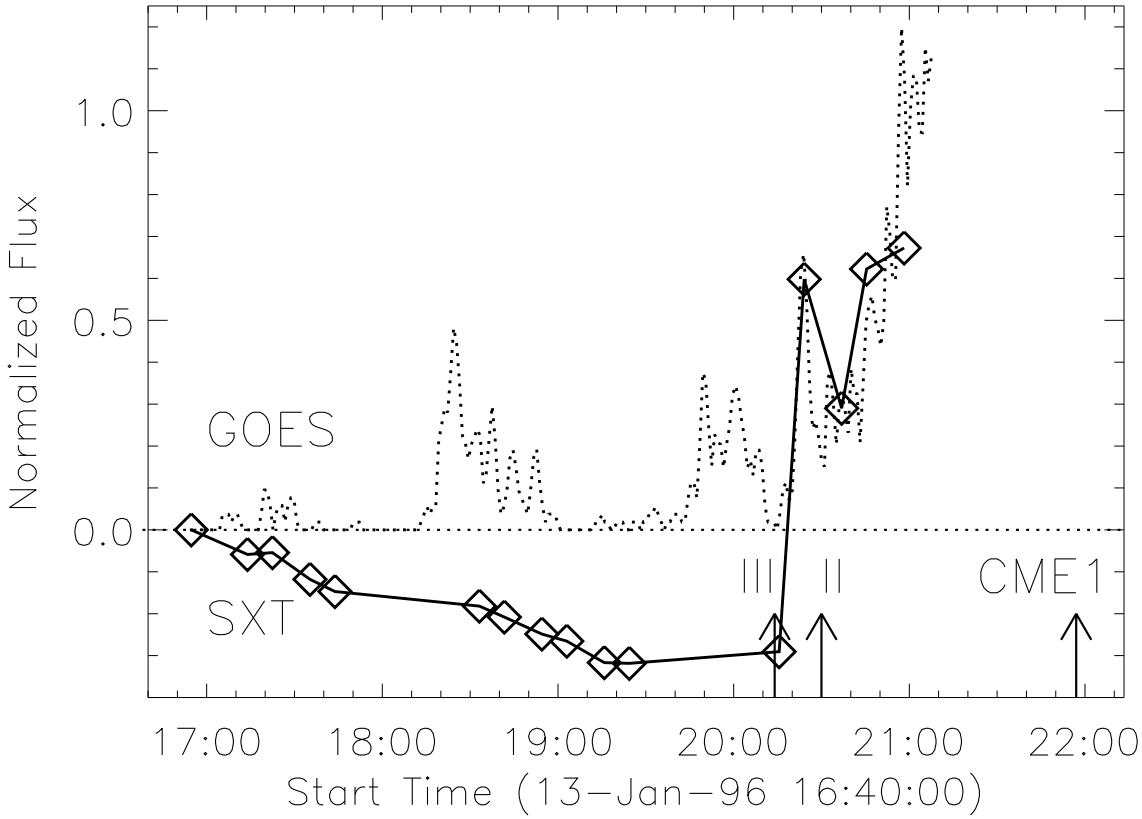

Figure 6: Soft X-ray light curve (solid curve with diamonds) obtained from *Yohkoh*/SXT images as compared to GOES X-ray light curve (dotted). The start times of the metric type II burst and the time the CME was first observed in the field of view of LASCO/C3 are marked. The horizontal dashed line represents the pre-event level in soft X-rays. SXT flux was normalized with respect to the value at 16:54 UT. Prolonged coronal dimming is evident in the SXT light curve for about 3 hours before the sharp rise corresponding to the X-ray ejecta. The two smaller spurts of activity seen in GOES light curve (at 18:30 and 20:00 UT) could not be compared with SXT data because they occurred during *Yohkoh* night.